Electronic Supplementary Material (ESI) for Journal of Materials Chemistry A.

An Organic-Inorganic Semi-Interpenetrating Network Ionogel Electrolyte for High-Voltage Lithium Metal Batteries

Anyu Su[a], Panlong Guo[b], Jian Li[b], Dongxiao Kan[a], Qiang Pang[b,c], Tianqi Li[b], Junqi Sun[b], Gang Chen[a,*], Yingjin Wei[a,*]

[a] Key Laboratory of Physics and Technology for Advanced Batteries (Ministry of Education), Jilin Engineering Laboratory for New Energy Materials and Technology, College of Physics, Jilin University, Changchun 130012, P. R. China
[b] State Key Laboratory of Supramolecular Structure and Materials, College of Chemistry, Jilin University, Changchun 130012, P. R. China
[c] School of Science, Dalian Maritime University, Dalian 116026, (P. R. China)

[*] Corresponding authors

Email: gchen@jlu.edu.cn (G. Chen), yjwei@jlu.edu.cn (Y. J. Wei)

Tel: 86-431-85155126

Table of Contents:

Figure S8. Galvanostatic cycling performance of Li/PIL-IL/Li symmetrical cell at 25 °C and 0.2 mA cm^{-2}.

Figure S9. (a) Cycling performance of LVP//Li full cell fabricated by commercial celgard 2320 separator and carbonate electrolyte at 0.5 C in 3.0- 4.3 V and 3.0-4.8 V. (b, c) Corresponding charge/discharge profiles in 3.0-4.3 V and 3.0–4.8 V, respectively.

Figure S10. Voltage profiles of the (a) $Li_3V_2(PO_4)_3$/PIL-GF-IL/Li, (b) $Li_3V_2(PO_4)_3$ /GF-IL/Li and (c) $Li_3V_2(PO_4)_3$ /PIL-IL/Li cells at various cycles.

Figure S11. Cycling performance of $Li_3V_2(PO_4)_3$/Li full cells using PIL-GF-IL ionogel and commercial electrolyte at 55 °C.

Table S2. Comparison of the electrochemical performances of the LVP/Li cells using the PIL-GF-IL ionogel electrolyte with the reported ionogel electrolytes[5–11].

Figure S12. EDS images of C, N, O, F, S elements of the lithium anode of LVP/GF-IL/Li cell after cycling.

Figure S13. EDS images of C, N, O, F and S elements of the lithium anode of LVP/GF-IL/Li cell after cycling.

Figure S14. Leakage experiment of PIL-GF-IL and GF-IL ionogels.

Figure S15. CV curves of the Li/PIL-GF-IL/Al, Li/PIL-IL/Al, and Li/GF-IL/Al cells at the sweep rate of 50 mV s^{-1}.

Figure S16. Al 1s XPS spectra of fresh Al foil.

Figure S17. SEM images of (a) fresh Al foil, and the Al current collector of (b) LVP/PIL-GF-IL/Li, (c) LVP/GF-IL/Li and (d) LVP/PIL-IL/Li full cells dissembled after cycling (insert: digital photographs).

Figure S18. (a,b) Cycling performance and charge/discharge profiles of NCM/PIL-GF-IL/Li cell at 0.5 C, respectively. (c,d) Cycling performance and charge/discharge profiles of LNMO/PIL-GF-IL/Li cell at 0.5 C, respectively.

1. Experimental Procedures

1.1 Materials: 1-vinylimidazole (VIm, 99%), lithium bis(trifluoromethanesulfonyl) imide (LiTFSI, 99%), 2-bromodiethyl ether (90%) were purchased from Sigma-Aldrich. 2, 2-azobisisobutyronitrile (AIBN, 99%) and 2-bromoethylamine hydrobromide (98%) were purchased from TCI Chemical. The VIm monomer was purified by passing them through an aluminium oxide column. Solvents including dimethyl sulfoxide (DMSO), ethanol, ether, acetone, chloroform, ethyl acetate were purchased from Beijing Chemical Works. Glycidyl polyhedral oligomeric silsesquioxane (GPOSS, AIKE REAGENT). Glass fiber (GF, Whatman, 1825-090).

1.2 Synthesis of $EtO(CH_2)_2MMI]TFSI$ ionic liquid: The synthesize of 1,2-dimethyl-3-ethoxyethyl imidazolium bis(trifluoromethane- sulfonyl)imide ($EtO(CH_2)_2MMI]TFSI$) ionic liquid with their structure shown in **Figure S3** were synthesized according to our previously reported protocol.[1] In brief, 2-Bromoethyl ethyl ether (3.06g, 0.02 mol) was added to 1,2-Dimethylimidazole (1.92 g, 0.02 mol) under stirring followed by incubating the reaction mixture under stirring at 80 °C for 4 h, resulting in the formation of solid crude products in the reaction mixture. The solid products (termed IL/Br) were purified via recrystallization and then dissolved in water to make an aqueous solution with a concentration of 20 mg/mL. The resultant aqueous solution was further added into an aqueous solution of LiTFSI (1 M). After stirring for 3 h, the mixture solution that had separated into two phases was transferred into a separate funnel and dichloromethane (100 mL) was added to extract the IL product. The dichloromethane phase was collected and washed with water for three times,

followed by removing the dichloromethane via rotary evaporation to obtain the IL products that were further dried in a vacuum oven at 100 °C for 24 h to get the final products (70% yield). IL/Br: ^{1}H-NMR(500 MHz, DMSO): 7.68 (d, 1H), 7.63 (d, 1H), 4.32 (t, 2H), 3.78 (s, 3H), 3.68 (t, 2H), 3.43 (q, 2H), 2.60 (s, 3H), 1.07 (t, 3H). IL/TFSI: ^{1}H-NMR(500 MHz, $CDCl_3$): 7.30 (d, 1H), 7.21 (d, 1H), 4.25 (t, 2H), 3.81 (s, 3H), 3.72 (t, 2H), 3.48 (q, 2H), 2.62 (s, 3H), 1.15 (t, 3H)

1.3 Synthesis of [EtVIm]Br monomer: 1-ethyl-3-vinylimidazolium bromide ([EtVIm]Br) was synthesized via the protocol reported previously.[2] Typically, bromoethane (2.73g, 0.025 mol), 1-vinylimidazole (2.35 g, 0.025 mol) and ethyl acetate (20 mL) were mixed in a 500 mL round-bottomed flask string at 30 °C for 48h. The resultant white solid was washed with ethyl acetate several times. The product was dried in a vacuum oven at 50 °C and white product was finally obtained (4.57 g, 90% yield). ^{1}H-NMR (500 MHz, D_2O), d (TMS, ppm): 8.97 (s, 1H), 7.69 (s, 1H), 7.52 (s, 1H), 7.08 (dd, 1H), 5.74 (dd, 1H), 5.36 (dd, 1H), 4.20 (m, 2H), 1.46 (m, 3H).

1.4 Synthesis of [AVIm]Br·HBr monomer: The [3-aminoethyl-1-vinylimidazolium]Br·HBr ([AVIm]Br·HBr) was synthesized according to the protocol reported previously.[3] Typically, 2-bromoethylamine hydrobromide (5.1 g, 0.025 mol), 1-vinylimidazole (2.35 g, 0.025 mol) and acetonitrile (20 mL) were mixed in a 500 mL round-bottomed flask, followed by stirring and refluxing the mixture at 30 °C for 48h. The resultant white solid was separated by filtration and then washed with anhydrous ethanol to remove the impurities. The product was dried in a vacuum oven at 50 °C and white product was finally obtained (80% yield). ^{1}H NMR (500 MHz, D_2O, TMS), d (TMS, ppm): 9.28 (s, 1H), 7.90 (s, 1H), 7.75 (s, 1H), 7.23 (dd, 1H), 5.91 (dd, 2H,), 5.53 (dd, 1H), 4.57 (m, 2H), 3.48 (m, 2H).

1.5 Synthesis of PIL-NH_2/TFSI copolymers: Firstly, the PIL-NH_2/Br copolymers were synthesized via AIBN-initiated free radical polymerization. In brief, the [AVIm]Br·HBr (0.30 g, 1.00mmol), [EtVIm]Br (1.83 g, 9.00 mmol), AIBN (0.15g, 0.91 mmol) and solvent mixture (5mL) of DMSO/water (3/2, v/v) were mixed in Schlenk tube. By using freeze-thaw method to degasses the mixture for three times, and then incubating the reaction tube in an oil bath under stirring at 70 ºC for 24 h. The crude products were purified by precipitation into acetone, and then dried under vacuum at 40 ºC for 48 h. The products were finally obtained (2.52 g, 82% yield). Secondly, PIL-NH_2/Br (2.22 g) and NaOH (0.40 g) were dissolved in deionized water (100 mL). Then the PIL-NH_2/Br aqueous solution was added into an aqueous solution of LiTFSI (3.44 g). Precipitation was obtained when adding the PIL-NH_2/Br aqueous solution into the LiTFSI aqueous solution, followed by stirring for 48 h. Then the precipitate was obtained via filtered and thoroughly washed with deionized water. The obtained filtrate was dried under vacuum at 80 ºC for 24 h (86% yield).

1.6 Preparation of PIL-GF-IL ionogel electrolytes: The PIL-GF-IL ionogel electrolytes with organic-inorganic semi-interpenetrating networks were prepared by a strategy as shown in Figure 1a of the main article. PIL-NH_2/TFSI (160 mg), IL (320 mg), LiTFSI (64 mg), and GPOSS (4.5 mg) were dissolved in acetone (1 mL). The glass fibers with a diameter of 18 mm were soaked in the acetone solution. Subsequently, place the glass fiber with acetone solution in an oven at 25 °C for 24 h, and then drying the resultant concentrated solution at 60 °C for 12 h and 105 °C for 12 h in a vacuum oven to crosslink PIL-NH_2/TFSI and evaporate acetone absolutely. The

ionogel electrolytes with organic-inorganic semi-interpenetrating networks were stored in an argon-filled glove box (H_2O < 0.1 ppm, O_2 < 0.1 ppm) for at least 72 h.

1.7 Preparation of PIL-IL ionogel electrolytes: The PIL-IL ionogel electrolytes were prepared as follows: PIL-NH_2/TFSI (160 mg), IL (320 mg), LiTFSI (64 mg), and GPOSS (4.5 mg) were dissolved in acetone (1 mL). Then the homogeneous solution was cast into cylindrical stainless steel mold. The solution was dried at room temperature for 24 h and then dried at 60 ºC for 48 h and 105 ºC for 12 h under vacuum. After peeling off from the stainless steel mold, a self-standing membrane was obtained. The ionogel electrolytes were stored in an argon-filled glove box (H_2O < 0.1 ppm, O_2 < 0.1 ppm) for at least 72 h.

1.8 Instruments and characterizations: ^{1}H-NMR (500 MHz) spectra were recorded on a Bruker Advance III spectrometer. Rheological measurements were carried out on a TA HR-2 rheometer with parallel plate geometry. The morphology and energy dispersive spectroscopy (EDS) of materials were studied on a Hitachi S-4800 field emission scanning electron microscopy (SEM). X-ray photoelectron spectroscopy (XPS) analysis was performed on a VG scientific ESCALAB 250 spectrometer. Digital images were captured with a Canon SX40 HS camera in macro mode. Thermal stabitliy analysis was determined on a TA Instruments Q500 thermogracimetric analyzer (TGA) under the nitrogen flow from 25 to 800 ºC with a heating rate of 10 ºC min^{-1}.

1.9 Electrochemical measurements: The IGEs' ionic conductivity was measured by impedance measurements on blocking stainless steel/IGEs/stainless steel cells using a Bio-Logic VSP electrochemical workstation at a frequency range of 10 Hz–100 kHz

with ac amplitude of 10 mV from 25 ºC to 80 ºC. The ionic conductivity was calculated according to the eqution of $\sigma=L/RS$. Where, R is the bulk electrolyte ohmic resistance; S the area of the ionogel electrolyte, and L the thickness of the electrolyte, which were 422±10, 443±20 and 420±10 μm for GF, PIL-GF-IL and GF-IL, respectively. The electrochemical impedance spectrum measurements were performed using the Bio-Logic VSP electrochemical workstation over a frequency range of 200 kHz to 0.1 Hz with ac amplitude of 10 mV. The transference number was calculated according to this equation:

$$t_+ = \frac{i_{ss}(\Delta V - i_0 R_0)}{i_0(\Delta V - i_{ss} R_{ss})} \quad (1)$$

Here, t_+ refers to the transference number of Li^+, ΔV (10 mV) is the applied voltage difference, i_0 and i_{ss} are the initial and steady state current, and R_0 and R_{ss} are the impedances before and after the measurements. Linear sweep voltammetry (LSV) was performed at 25 ºC at scan rate of 1.0 mV s^{-1} using a stainless steel/IGEs/Li cell. Li plating/stripping tests were measured on a symmetrical Li/IGEs/Li cell using a Land-CT2001A battery tester under a constant current density of 0.2 mA cm^{-2}. Galvanostatic charge-discharge experiments were performed on a Land-2001 automatic battery tester.

1.10 Fabrication and measurement of lithium metal batteries: The $Li_3V_2(PO_4)_3$ (LVP) cathode material was prepared by the sol-gel method as shown in our previous report[4]. The LVP cathode electrode was prepared by mixing LVP, Super P conductive additive and poly(vinylidene) fluoride (PVDF) with a weight ratio of 75:15:10 and then pasting onto aluminum foil current conductor, followed by drying at 120 ^oC overnight in a vacuum oven. The LVP/IGE/Li cell was assembled in type 2032 coin cell to form

a solid-state battery. The LVP/IGE/Li coin cells collected after the galvanostatic experiment were disassembled in a glovebox. The commercial electrolyte was 1M $LiPF_6$ dissolved in ethylene carbonate (EC), dimethyl carbonate (DMC) and ethyl methyl carbonate (EMC) with EC: DMC: EMC = 1:1:1 by v/v ratio. The working and counter electrodes were separated by a Ceglard 2320 membrane.

2. Figures and Tables

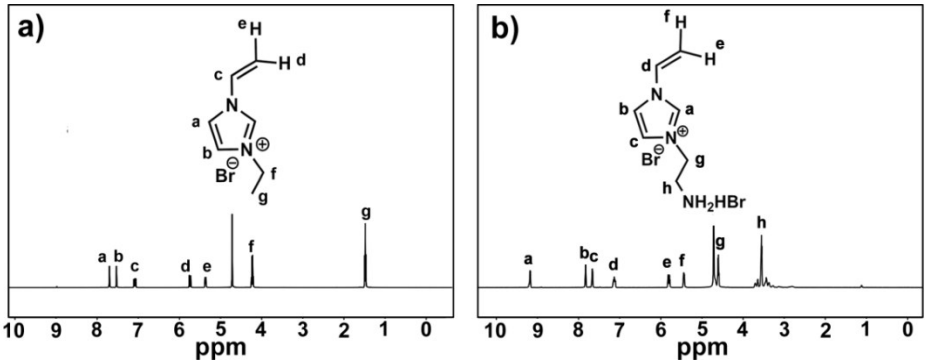

Figure S1. ^{1}H NMR spectra of the (a) [EtVIm]Br and (b) [AVIm]Br·HBr.

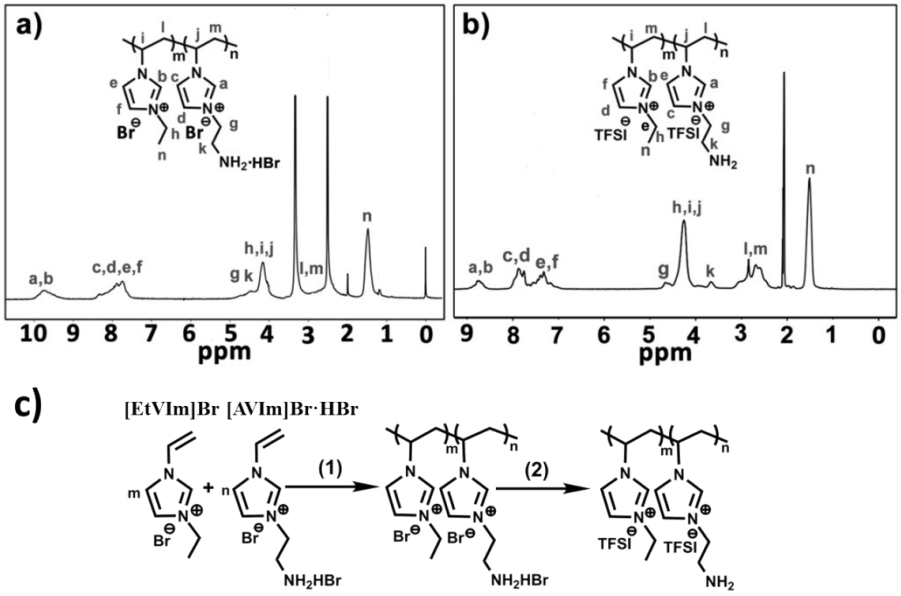

Figure S2. ^{1}H NMR spectra of the (a) PIL-NH_2/Br and (b) PIL-NH_2/TFSI. (c) Schematic of PIL-NH_2/TFSI copolymer.

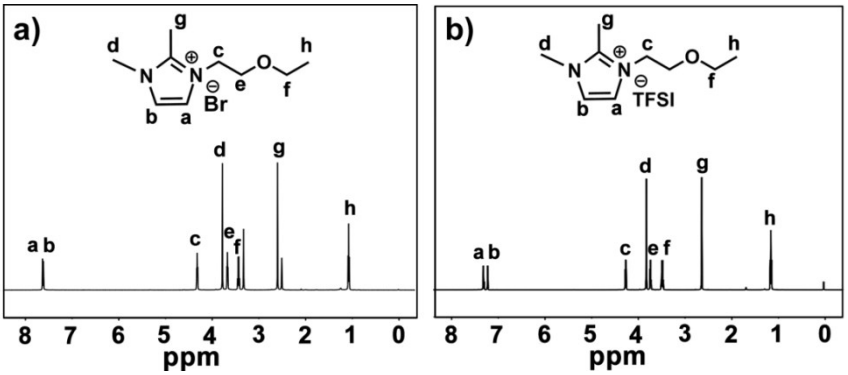

Figure S3. ^{1}H NMR spectra of the (a) IL/Br and (b) [$EtO(CH_2)_2$MMI]TFSI ionic liquid.

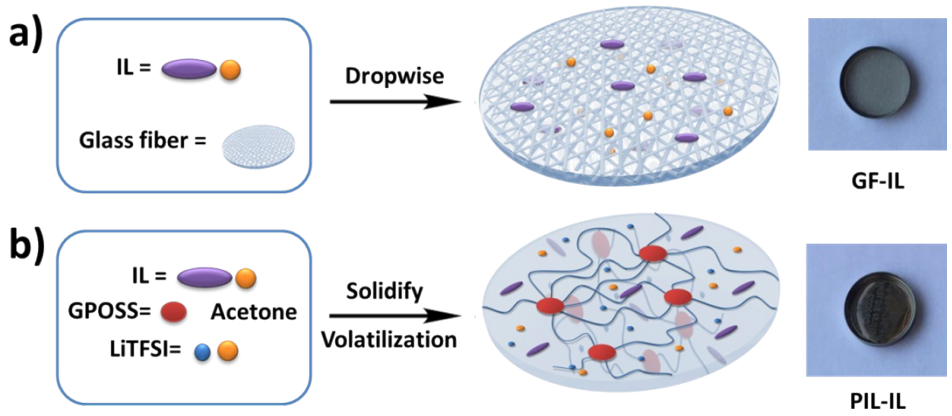

Figure S4. Schematic of the synthesis of the (a) GF-IL and (b) PIL-IL ionogels (insert: digital photographs)

Table S1. Active energy (E_a) and ionic conductivity of PIL-GF-IL, GF-IL and PIL-IL ionogels.

Samples	Ionic Conductivity (10^{-3} S cm^{-1})						E_a (kJ mol^{-1}) (25-80 °C)
	25 °C	40 °C	50 °C	60 °C	70 °C	80 °C	
PIL-GF-IL	0.557	0.891	1.22	1.27	1.73	2.43	23.57
GF-IL	4.28	5.45	8.1	12.7	13.7	18.4	26.44
PIL-IL	1.27	1.68	2.225	3.33	4.45	5.56	26.94

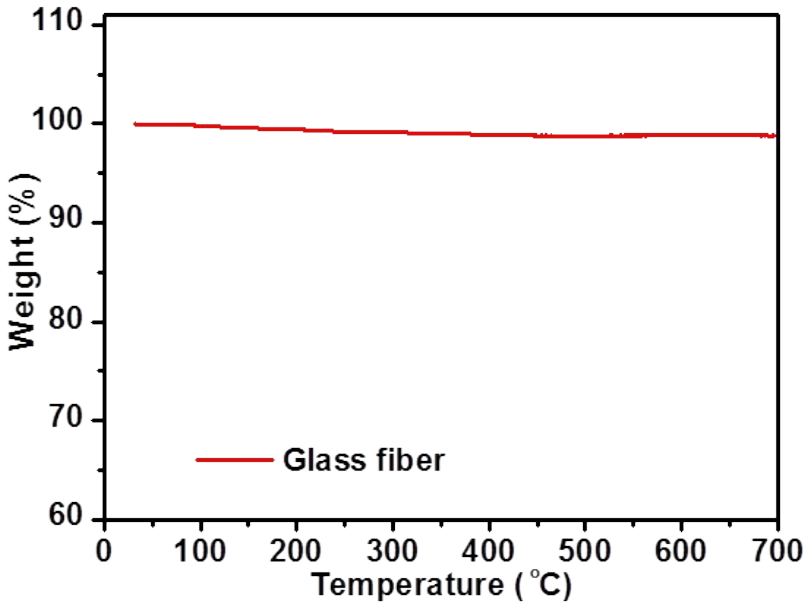

Figure S5. TGA curve of glass fiber.

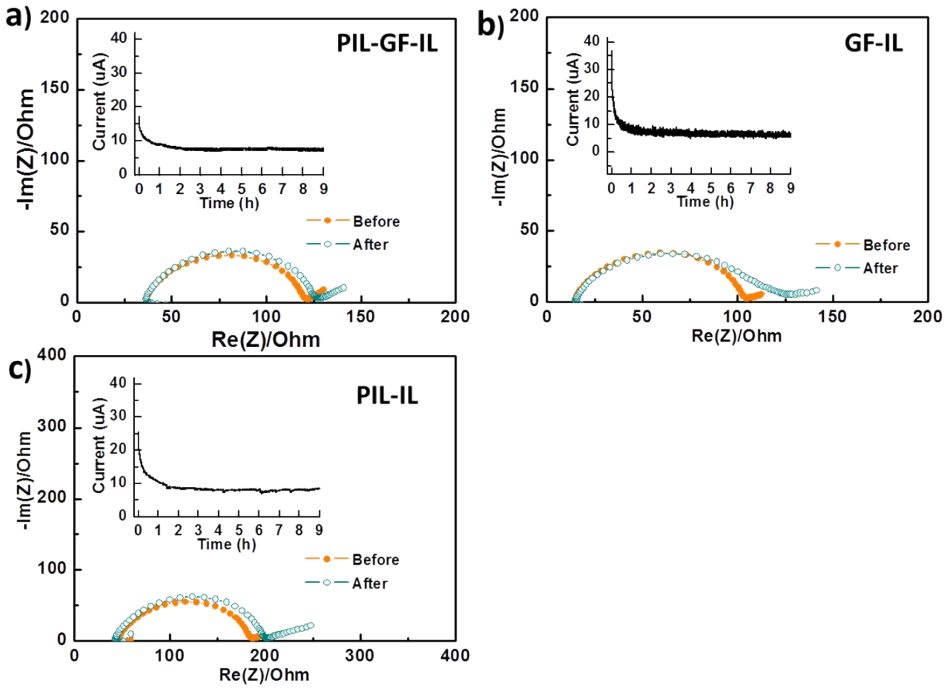

Figure S6. EIS of Li symmetric cells using (a) PIL-GF-IL, (b) GF-IL and (c) PIL-IL as electrolyte before and after polarization. The inserts show the variation of current with time during polarization at an applied voltage of 10 mV at 25 °C.

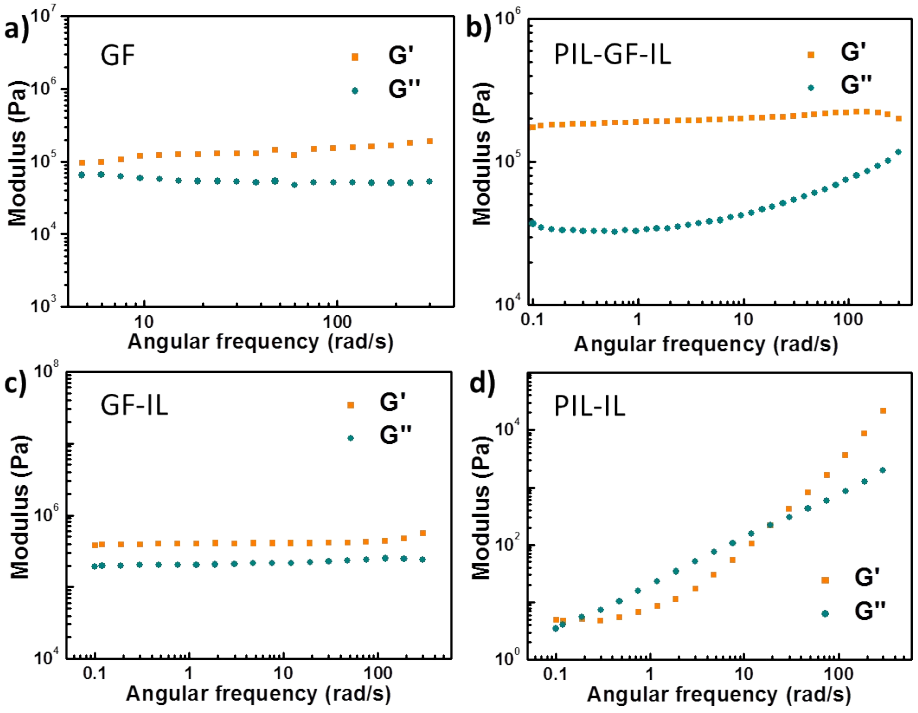

Figure S7. Frequency dependence of the storage (G') and loss (G'') modulus of the (a) GF, (b) PIL-GF-IL, (c) GF-IL and (d) PIL-IL at 25 °C.

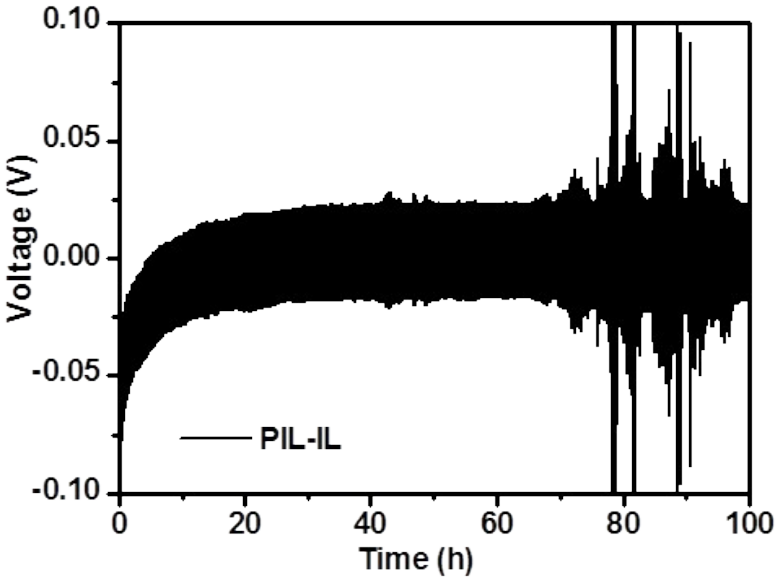

Figure S8. Galvanostatic cycling performance of Li/PIL-IL/Li symmetrical cell at 25 °C and 0.2 mA cm^{-2}.

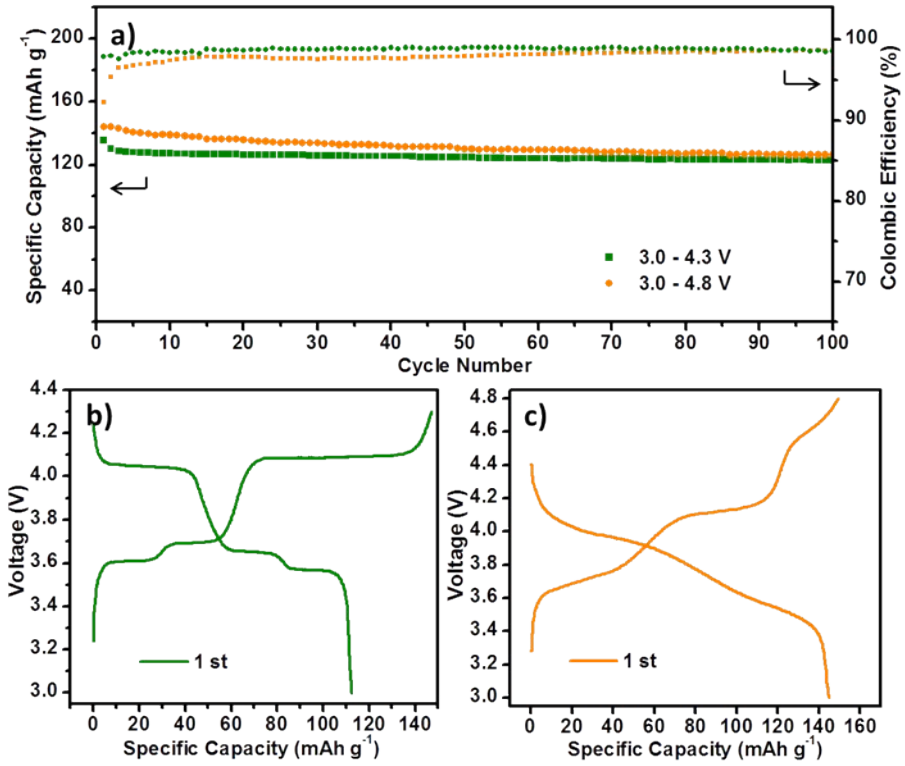

Figure S9. (a) Cycling performance of LVP//Li full cell fabricated by commercial celgard 2320 separator and carbonate electrolyte at 0.5 C in 3.0- 4.3 V and 3.0-4.8 V. (b, c) Corresponding charge/discharge profiles in 3.0-4.3 V and 3.0–4.8 V, respectively.

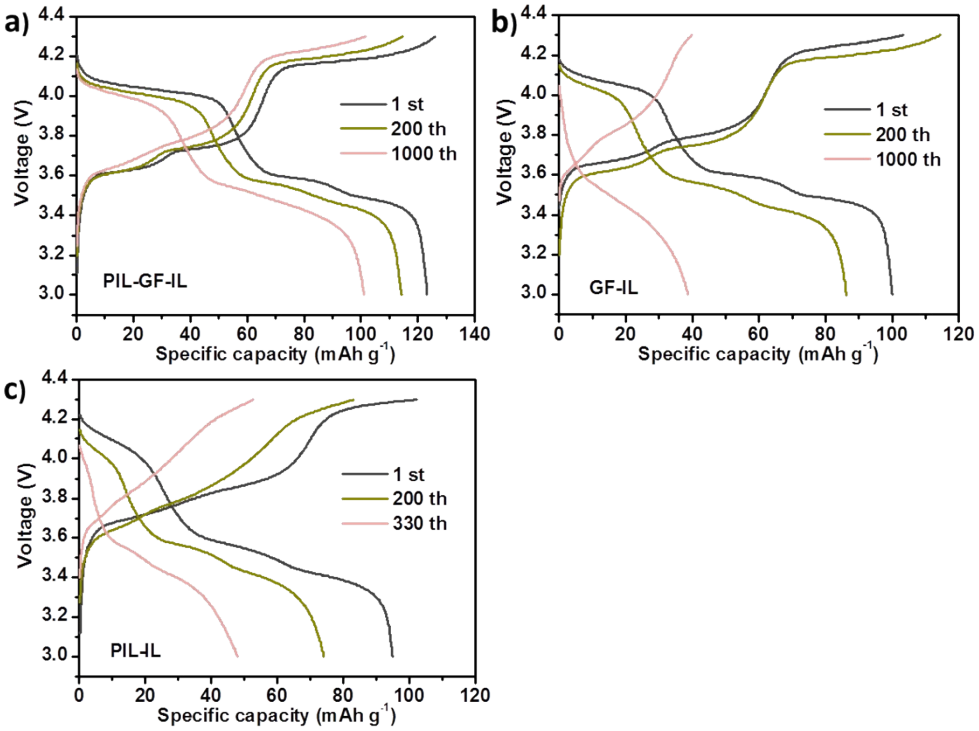

Figure S10. Voltage profiles of the (a) $Li_3V_2(PO_4)_3$/PIL-GF-IL/Li, (b) $Li_3V_2(PO_4)_3$ /GF-IL/Li and (c) $Li_3V_2(PO_4)_3$ /PIL-IL/Li cells at various cycles.

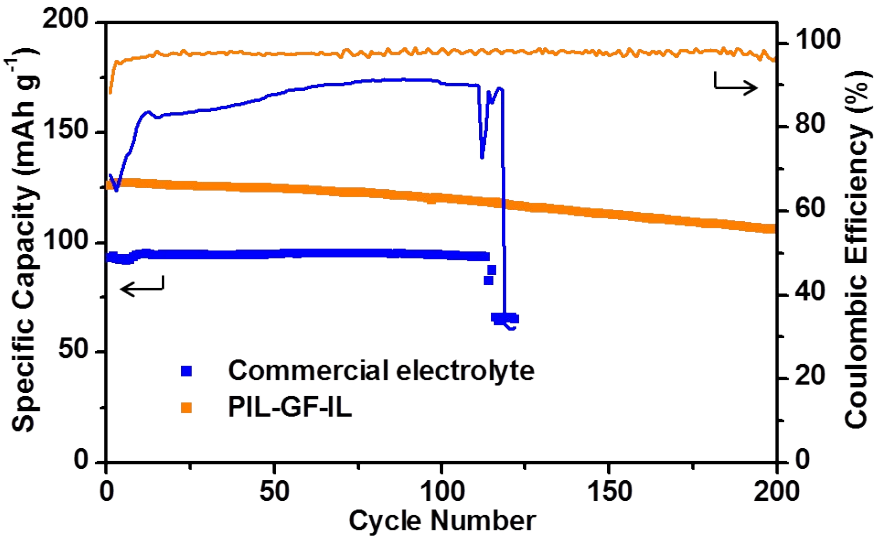

Figure S11. Cycling performance of $Li_3V_2(PO_4)_3$/Li full cells using PIL-GF-IL ionogel and commercial electrolyte at 55 °C.

Table S2. Comparison of the electrochemical performances of the LVP/Li cells using the PIL-GF-IL ionogel electrolyte with the reported ionogel electrolytes[5–11].

Electrolyte	Cell component	Voltage (V)	Discharge capacity (mAh/g)	Cycles/ Retention	Ref.
PIL-GF-IL	LVP//Li	3.0 - 4.3	123 (0.5 C)	1000 (83%)	**Our work**
		3.0 - 4.8	155 (0.5 C)	100 (91%)	
Li-IL@MOF	LFP//Li	2.0 - 4.2	145 (0.1 C)	100 (91%)	S5
PDADMAFSI/ LiFSI	LFP//Li	2.5 - 3.75	158 (C/15)	30 (100%)	S6
	NMC111/Li	3.0 - 4.3	150 (1.0 C)	50 (85%)	
PIN@LiTFSI-EMIMTFSI	LFP//Li	2.0 - 4.0	146 (0.1 C)	15 -	S7
PIN@LiTFSI-DEMETFSI	LFP//Li	3.0 - 4.4	155 (0.1 C)	200 -	S8
	LCO//Li	3.0 - 4.4	130 (0.1 C)	100 -	
Biomimetic Ant-nest Ionogel	LFP//Li	3.0 - 4.2	152 (0.1 C)	- -	S9
	NCM111//Li	2.8 - 4.2	145 (0.1 C)	- -	
ILE/SCA	LFP//Li	2.5 – 4.2	155 (0.1 C)	- -	S10
POSS-IL-LiTFSI	LFP//Li	2.5 – 3.9	154 (0.1 C)	65 (~91%)	S11

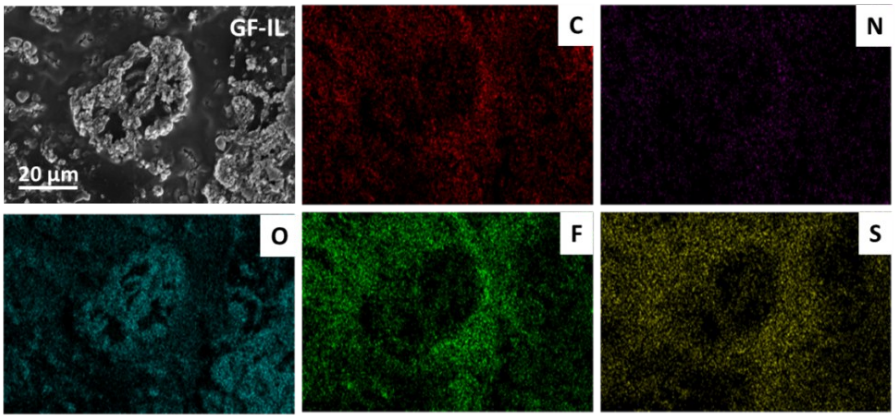

Figure S12. EDS images of C, N, O, F, S elements of the lithium anode of LVP/GF-IL/Li cell after cycling.

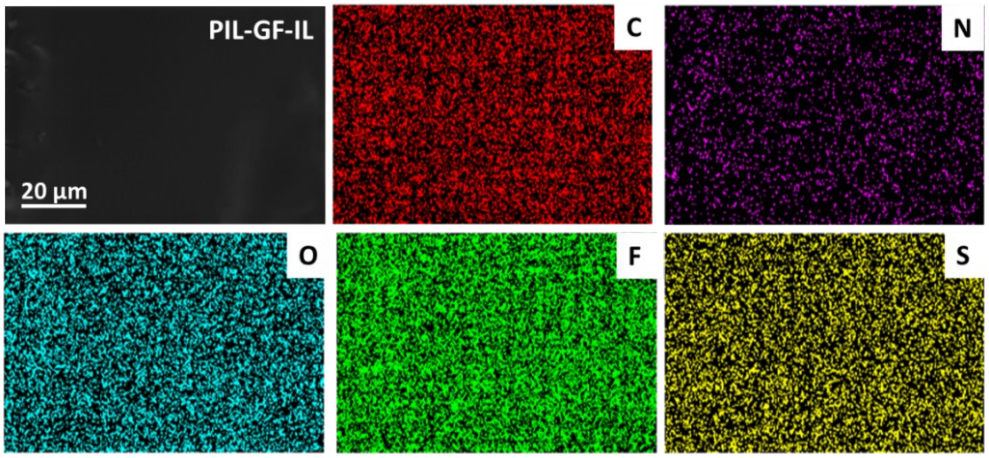

Figure S13. EDS images of C, N, O, F and S elements of the lithium anode of LVP/GF-IL/Li cell after cycling.

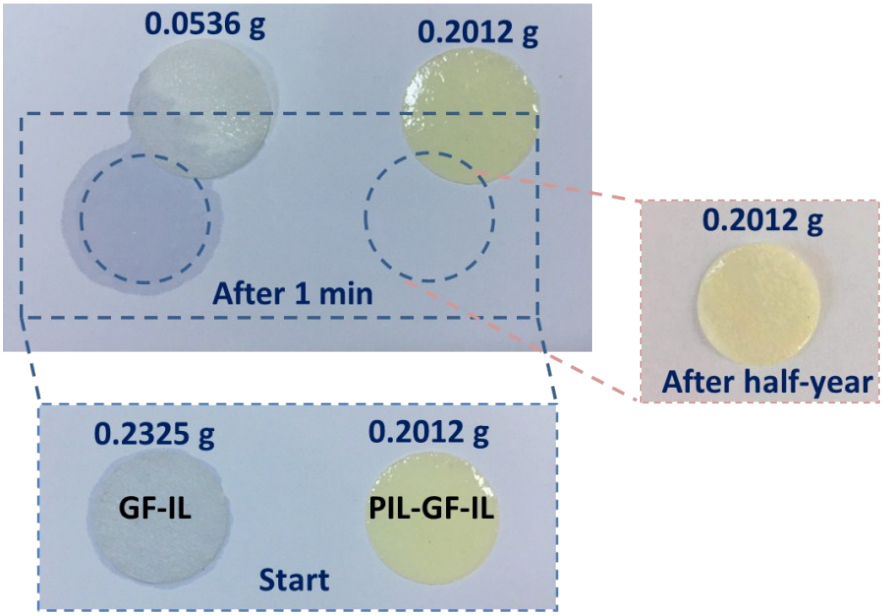

Figure S14. Leakage experiment of PIL-GF-IL and GF-IL ionogels.

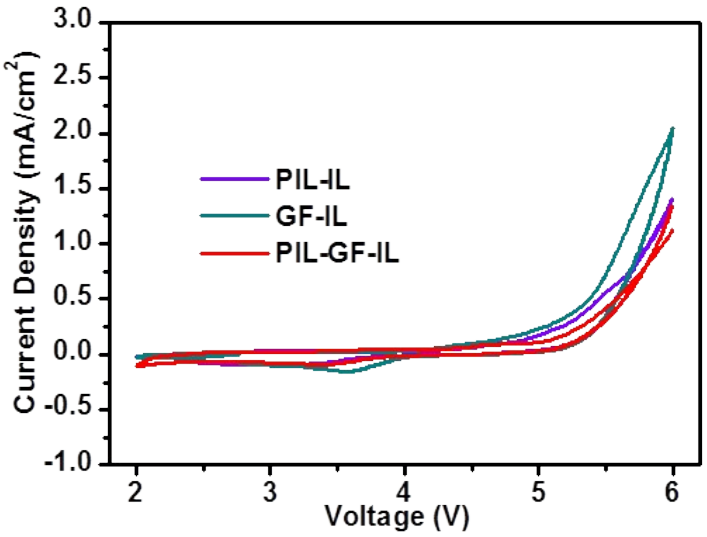

Figure S15. CV curves of the Li/PIL-GF-IL/Al, Li/PIL-IL/Al, and Li/GF-IL/Al cells at the sweep rate of 50 mV s^{-1}.

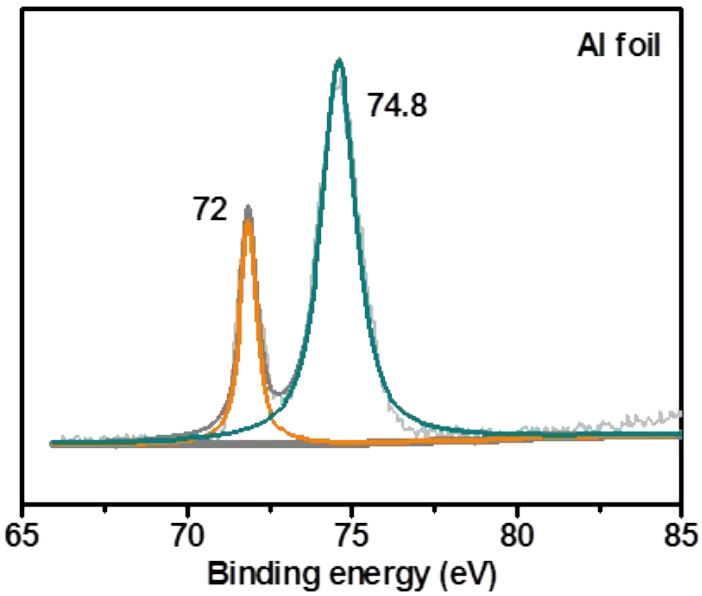

Figure S16. Al 1s XPS spectra of fresh Al foil.

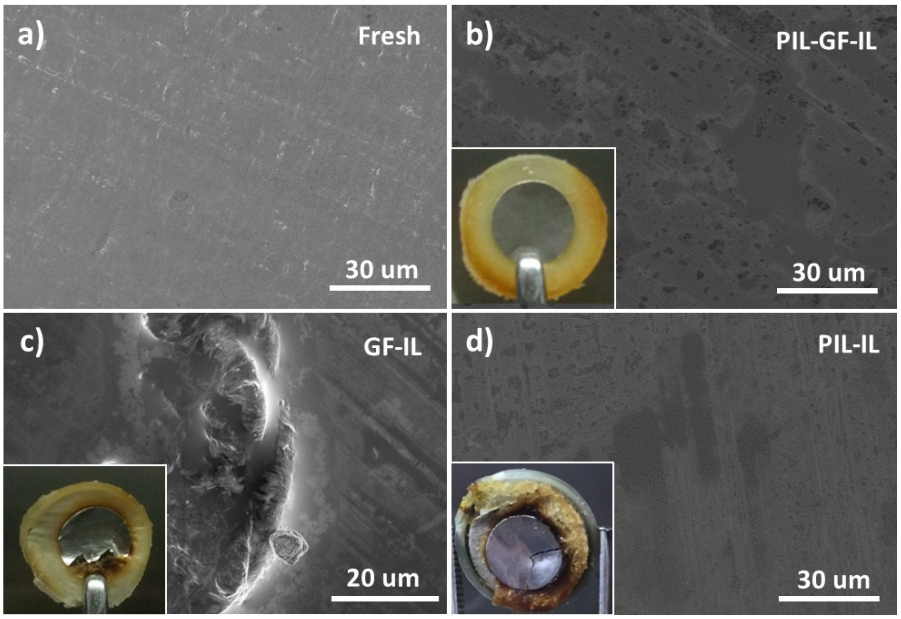

Figure S17. SEM images of (a) fresh Al foil, and the Al current collector of (b) LVP/PIL-GF-IL/Li, (c) LVP/GF-IL/Li and (d) LVP/PIL-IL/Li full cells dissembled after cycling (insert: digital photographs).

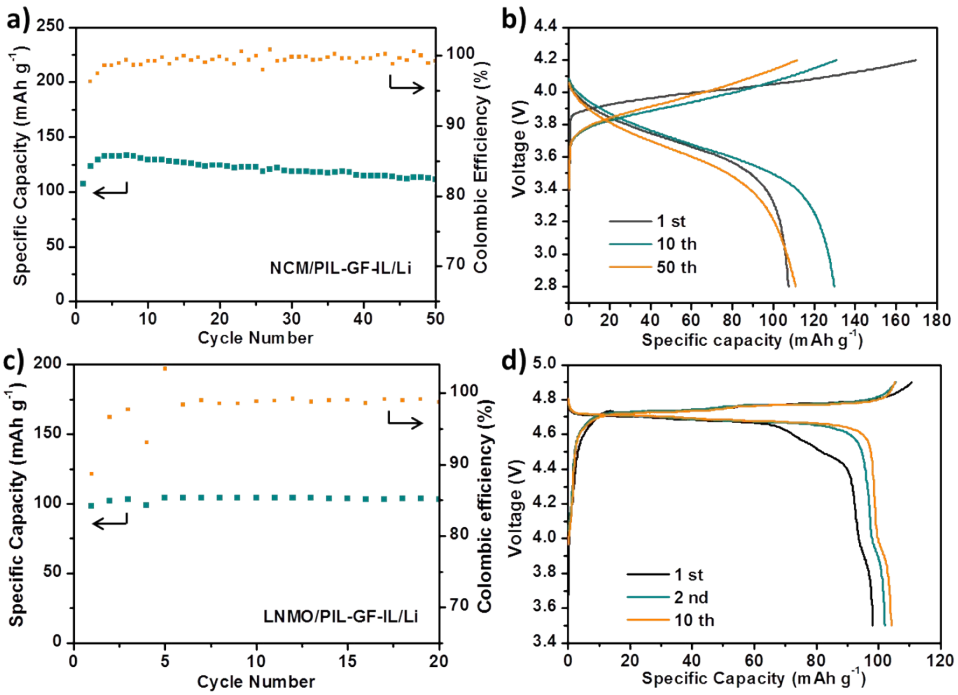

Figure S18. (a,b) Cycling performance and charge/discharge profiles of NCM/PIL-GF-IL/Li cell at 0.5 C, respectively. (c,d) Cycling performance and charge/discharge profiles of LNMO/PIL-GF-IL/Li cell at 0.5 C, respectively.

3. References

[1] P. Guo, A. Su, Y. Wei, X. Liu, Y. Li, F. Guo, J. Li, Z. Hu, J. Sun, *ACS Appl.Mater. Interfaces.* 2019,11,21,19413-19420.

[2] E.D. Bates. R.D. Mayton, I. Ntai, J.H. Davis, Jr. *J. Am. Chem. Soc.* 2002, *124*, 926.

[3] M. J. Monteiro, F. F. Camilo, M. C. C. Ribeiro, R. M. Torresi, *J. Phys. Chem. B,* 2010, *114*, 12488.

[4] A. Su, Q. Pang, X. Chen, J. Dong, Y. Zhao, R. Lian, D. Zhang, B. Liu, G. Chen, Y. Wei, J. Mater. Chem. A. 2018, 6, 23357.

[5] Z. Wang, R. Tan, H. Wang, L. Yang, J. Hu, H. Chen and F. Pan, Adv. Mater., 2018, 30, 1704436.

[6] X. Wang, F. Chen, G. M. A. Girard, H. Zhu, D. R. MacFarlane, D. Mecerreyes, M. Armand, P. C. Howlett and M. Forsyth, Joule, DOI: 10.1016/j.joule.2019.07.008.

[7] P. Zhang, M. Li, B. Yang, Y. Fang, X. Jiang, G. M. Veith, X.-G. Sun and S. Dai, Adv. Mater., 2015, 27, 8088–8094.

[8] X. Tian, Y. Yi, P. Yang, P. Liu, L. Qu, M. Li, Y. Hu and B. Yang, ACS Appl. Mater. Inter., 2019, 11, 4001–4010.

[9] N. Chen, Y. Dai, Y. Xing, L. Wang, C. Guo, R. Chen, S. Guo and F. Wu, Energy Environ. Sci., 2017, 10, 1660–1667.

[10] F. Wu, N. Chen, R. Chen, L. Wang and L. Li, Nano Energy, 2017, 31, 9–18.

[11] G. Yang, C. Chanthad, H. Oh, I. A. Ayhan and Q. Wang, J. Mater. Chem. A, 2017, 5, 18012–18019.